The final publication is available at

http://dx.doi.org/10.1021/am405939y

Additional Information

# Polymer composites containing gated mesoporous materials for on-command controlled release

Carolina Acosta,[*a,b] Edgar Pérez-Esteve,[a,b] Carlos A. Fuenmayor,[d] Simona Benedetti,[d] Maria Stella Cosio,[d] Juan Soto,[b] Félix Sancenón,[b,c] Saverio Mannino,[d] José Barat,[a] María D. Marcos,[b,c] Rámon Martínez-Máñez.[b,c]

[a] Grupo de Investigación e Innovación alimentaria (CUINA) - Universidad Politécnica de Valencia
[b] Centro de Reconocimiento Molecular y Desarrollo Tecnológico (IDM) - Unidad Mixta: Universidad de Valencia & Universidad Politécnica de Valencia.
[c] CIBER de Bioingeniería, Biomateriales y Nanomedicina (CIBER-BBN).
[d] Department of Food, Environmental and Nutritional Sciences – DeDENS. University of Milan

KEYWORDS: Composites, On-command delivery, Mesoporous, Electrospun nanofibers, Hybrid material

ABSTRACT Polyamidic nanofibrous membranes containing gated silica mesoporous particles, acting as carriers, are described as novel hybrid composite materials for encapsulation and on-command delivery of garlic extracts. The carrier system consists of MCM-41 solids functionalized in the outer surface, with linear polyamines (Solid **P1**) and with hydrolyzed starch (Solid **P2**), both acting as molecular gates. Those particles were adsorbed on electospun nylon-6 nanofibrous membranes yielding to composite materials **M1** and **M2**. FE-SEM analysis confirmed the presence of particles incorporated on the nylon nanofibers. The release of the entrapped molecules (garlic extract) from the **P1**, **P2**, **M1** and **M2** materials was evaluated using

cyclic voltammetry measurements. Electrochemical studies showed that at acidic pH **P1** and **M1** were unable to release their entrapped cargo (closed gate), whereas at neutral pH both materials release their loading (open gate). Dealing with **P2** and **M2** materials, in the absence of pancreatin a negligible release is observed (closed gate), whereas in the presence of enzyme the load is freely to diffuse to the solution. These newly developed composite nanomaterials, provide a homogeneous easy-to-handle system with controlled delivery and bioactive-protective features, having potential applications on pharmacology, medical and engineering fields

INTRODUCTION

In the last years, anchoring organic or biological molecules on certain inorganic supports has resulted in the design of hybrid materials which show advanced cooperative functional behaviors.[1-2] One appealing concept in this area is related with the design of gated supports for advanced delivery applications.[3-4] These new materials contain switchable molecular-based entities which control the on-command release of previously entrapped guests. These gated materials are based on the combination of two components: (i) a suitable inorganic support acting as a container (for loading the cargo) and (ii) a switchable "gate-like" ensemble able to be "opened" upon the application or the presence of a predefined stimulus.[5] Selection of both components is important and determines the controlled release performances of the final support.

As inorganic scaffolds, mesoporous silica of different pore sizes and morphologies have been widely used.[6-8] Mesoporous supports can be prepared in different forms (from nanometric to micrometric) with tailor-made pores in the 2-10 nm range. Moreover they have a very high specific surface area (up to 1200 $m^2g^{-1}$), have homogeneous porosity, high inertness, a large loading capacity and are easy to functionalize.[9] These properties make silica mesoporous structures ideal candidates as scaffolds for delivery applications. In relation to the gated

ensemble, currently several molecular, supramolecular and nanoparticulated systems have been used. Those systems are able to deliver the entrapped cargo using several external stimuli such as light,[10-11] pH,[12-13] changes in redox potential,[14-15] temperature[16-17] and the presence of certain ions, molecules or biomolecules.[18-20]

In particular, the design of gated mesoporous materials have proved to be a promising starting point for applying the versatility of molecular and supramolecular concepts to the design of gating solids, and a way of studying the factors that can influence the design of molecular gating functions with advanced delivery functionalities. These concepts contrast with the design of traditional delivery systems which are often based on simple diffusion controlled processes.[21]

On the other hand, nanofibers are especially appealing for the development of novel composites with potential applications on areas such as vascularization, cell migration and attachment processes.[22-24] There are a number of different processing techniques used for the synthesis of nanofibers including drawing, self-assembly or phase separation, however electrospining is probably the most widely studied.[25] Electrospun nanofibers have surface properties that can be specially tailored to adjust and control porosity, composition and morphology, with a highly controllable three-dimensional structure and high surface area-to-volume ratios, for providing support on the inclusion of antimicrobial agents, drugs, flavors, colors, antioxidants, enzymes and other functional compounds.[26-28] Nanofibers have also been used in delivery applications, however there are few examples where release only occurs triggered by specific and selected stimuli and as stated above, sustained delivery is still the most common principle.

Very recently, nanofibers that incorporate different types of silica mesoporous materials have been prepared and characterized.[29-31] However, in these papers only the synthesis and the physical properties of the prepared fabrics are studied.

Taking into account the above mentioned facts we believe that a new range of potential applications can be envisioned by the combination of nanofibers to support gated silica mesoporous particles in order to obtain composites with the potential ability to deliver a certain cargo upon the application of target stimuli while cargo is protected until its specific delivery. In order to achieve this goal and as a proof of concept we have selected for this particular work two mesoporous systems able to protect and deliver the cargo upon changes in the pH or in the presence of a target enzyme (*vide infra*).[32-33] Those mesoporous scaffolds are then supported on nylon-6 nanofibers to provide a homogenous material for delivery.

As cargo we selected a garlic extract whose bioactive components have been reported to have antimicrobial, antiatherosclerotic and antioxidative properties.[34-35] Garlic extract contain among other substances allicin and diallyl disulfide, organosulfurs responsible of the functional properties of garlic. However, some of these functional compounds from garlic extract are unstable and have sensorial trouble for certain applications. In this context, the design of supports able to protect the cargo and induce delivery on-command is of importance.

EXPERIMENTAL PROCEDURE

All chemicals were purchased at the highest grade available and used directly without any further purification. Diallyldisulfide (tech., 80%) and NaClO4 (ACS Reagent, 98%) were purchased from Sigma Aldrich, NaBr was purchased from May and Baker Ltd, UK. All solutions were prepared with acetonitrile (HPLC Gradient grade, Fisher Scientific) and deionized water of

resistivity not less than 18.2 MU/cm-1 at 298 K (Millipore UHQ, Vivendi, UK). The chemicals nylon-6, formic acid (98%), tetraethylorthosilicate (TEOS), n-cetyltrimethylammonium bromide (CTAB), sodium hydroxide, triethanolamine (TEAH3), 3-aminopropyltriethoxysilane, 3-[2-(2-aminoethylamino) ethylamino]-propyl-trimethoxysilane and pancreatin from porcine pancreas were provided by Aldrich. The hydrolyzed starch Glucidex@ 47 (5% glucose, 50% maltose, 45% oligosaccharides and polysaccharides) was provided by Roquette.

Synthesis of mesoporous silica microparticles MCM-41

The mesoporous MCM-41 support, was first synthesized by "atrane route"[36] in which 4.68 g of CTAB was added at 118 °C to a solution of TEAH3 (25.79 g) containing 0.045 mol of a silatrane derivative (TEOS, 11 mL). Next 80 mL of water was slowly added with vigorous stirring at 70 °C. After a few minutes, a white suspension was formed. This mixture was aged at room temperature overnight. The resulting powder was collected by filtration and washed. Solid was dried at 70 °C and finally, in order to remove the template phase was calcined at 550 °C for 5 h using an oxidant atmosphere.

Synthesis of starch derivative (**Glu-N1**)

A solution of 3-aminopropyltriethoxysilane (**N1**, 5.85 mL, 25 mmol) was added to a suspension of hydrolyzed starch (Glucidex@ 47) in ethanol. The reaction mixture was stirred for 24 h at room temperature and heated at 60 °C for 30 min. The solvent was evaporated under reduced pressure.

Garlic bioactive compounds extraction

Garlic was obtained in local market. The garlic cloves were peeled and chopped. A certain amount of acetonitrile was used to crush the garlic and get a sample with a garlic acetonitrile

relation of 1:10 w/v where principal organosulfures were extracted. Solution was shaken by vortex for 3-5 min and then filtered and kept at 4 °C.

Garlic bioactive compounds loading (**P0**)

100 mg of mesoporous particle MCM-41 were suspended in 40 mL of garlic acetonitrile extract inside a round-bottom flask. The mixture was stirred for 24 h at room temperature. This mixture was filtered and dried at room temperature for 12 h.

Synthesis of **P1**

An excess of 3-[2-(2-aminoethylamino)-ethylamino]-propyl-trimethoxysilane (**N3**, 0.43 mL) was added to 0.1 g **P0** in 40 ml acetonitrile. The final mixture was stirred for 5.5 h at room temperature in an inert atmosphere of nitrogen. Solid was filtered and washed with acid solution at pH 2.0 (acidified with sulfuric acid) and dried for 12 h at 35 ºC.

Synthesis of **P2**

**Glu-N1** was added to **P0** in a 1:1 w/w relation. The final mixture was stirred for 5.5 h at room temperature under argon. The solid was filtered and washed with deionised water, and dried at for 12 h at 35 ºC.

Particles immobilization – Composites **M1** and **M2**

Polymer solution was made with 8 g of nylon-6 pellets dissolved in 26.6 mL of a formic acid (88 %) aqueous solution. The dispersion obtained was stirred for about 24 h to make a clear sol–gel. Then 80 mg of solid (**P1** for membrane **M1** and **P2** for membrane **M2**) were added and stirred for 5 h at 300 rpm. 5 mL syringe (Hamilton) was filled with the entire composite polymer solution and placed in a KDP100 syringe pump (KD-Scientific) at a flow rate of 0.20 mL min$^{-1}$. The needle of the syringe was linked to the Spellman SL150 high voltage power supply by an alligator clip, while a copper lamina, positioned at 11 cm in front of the needle, was used as

collector and grounded. The electrical potential was set at 25 kV. Production time of a single membrane was stopped at 10 min.

Release studies

Aqueous suspensions of the four materials were stirred for 5 h at 200 rpm. Each hour an aliquot from solution was taken, passed through nylon 0.45 um filters and then evaluated by cyclic voltammetry. Delivery sample was constituted by 12 mg of solid **P1** or **P2** and 30 cm$^2$ for **M1** or **M2** and suspended in 30 mL of the corresponding release solution. Delivery studies of solid **P1** and membrane **M1** were carried out in aqueous solution containing sulfate anion ($10^{-2}$ M) and at pH 7.0 and pH 2.0. Solid **P2** and membrane **M2** were suspended in aqueous solutions at pH 7.0 in the absence and in the presence of pancreatin.

Cyclic voltammetry

A CHI 1010 Electrochemical Analyzer (CH Instruments, Austin Texas) with a three electrode setup consisting of a glassy carbon working electrode, platinum auxiliary electrode and an Ag/AgCl reference electrode was employed. Cyclic voltammogram experiments were acquired with a scan rate of 50 mVs$^{-1}$ and were obtained by running a series of FIA. Experiments in which the potential was stepped incrementally from -0.1 to +1.5 V (vs. Ag/AgCl) and the current was measured.

Experiments were performed in aqueous reference solution with acetonitrile (50:50), sodium bromide 15 mM in 0.1 M of sodium perchlorate.[37] The measure solution has a 1:1 v/v ratio between reference solution (blank) and sample.

Characterization of materials

PXRD measurements were performed on a Seifert 3000TT diffractometer using CuKα radiation. Field Emission Scanning Electron Microscope images were acquired by FE-SEM ULTRA 55-

44-22, evaluated by secondary (SE2) and backscattered electrons (AsB) detectors. Samples were coated with platinum and examined at 5kV. An X-ray EDS detector was used for qualitative elements analysis. Dynamic Light Scattering (DLS) studies were conducted at 25 °C using a Malvern Zetasizer Nano ZS. Back-scattered light was detected at 173°, and the mean particle diameter was calculated from the quadratic fitting of the correlation function over 3 runs of 10 s duration. All measurements were performed in triplicate on previously sonnicated highly dilute aqueous dispersions. Thermogravimetric analyses were carried out on a TGA/SDTA 851e Mettler Toledo balance, using an oxidant atmosphere (air, 80 mLmin$^{-1}$) with a heating program consisting of a heating ramp of 10 °C per minute from 393 to 1273 K and an isothermal heating step at this temperature for 30 min. TEM images were obtained with a 100 kV Philips CM10 microscope. N2 adsorption-desorption isotherms were recorded with a Micromeritics ASAP2010 automated sorption analyzer. The samples were degassed at 120 °C in vacuum overnight. The specific surface areas were calculated from the adsorption data in the low pressure range using the BET model.[38]

RESULTS AND DISCUSSION

The gated materials

In this approach, MCM-41 was used as inorganic scaffold in the form of microparticles. The prepared MCM-41 support contains mesopores in the 2-3 nm range which allow the encapsulation of certain guests. In relation to the capping component two previously reported gates were selected; one based in the use of linear polyamines (for the preparation of **P1** material)[33] and other based in the use of hydrolyzed starch (for the preparation of **P2** material).[32] Scheme 1 shows the proposed paradigm for the preparation of the gated materials.
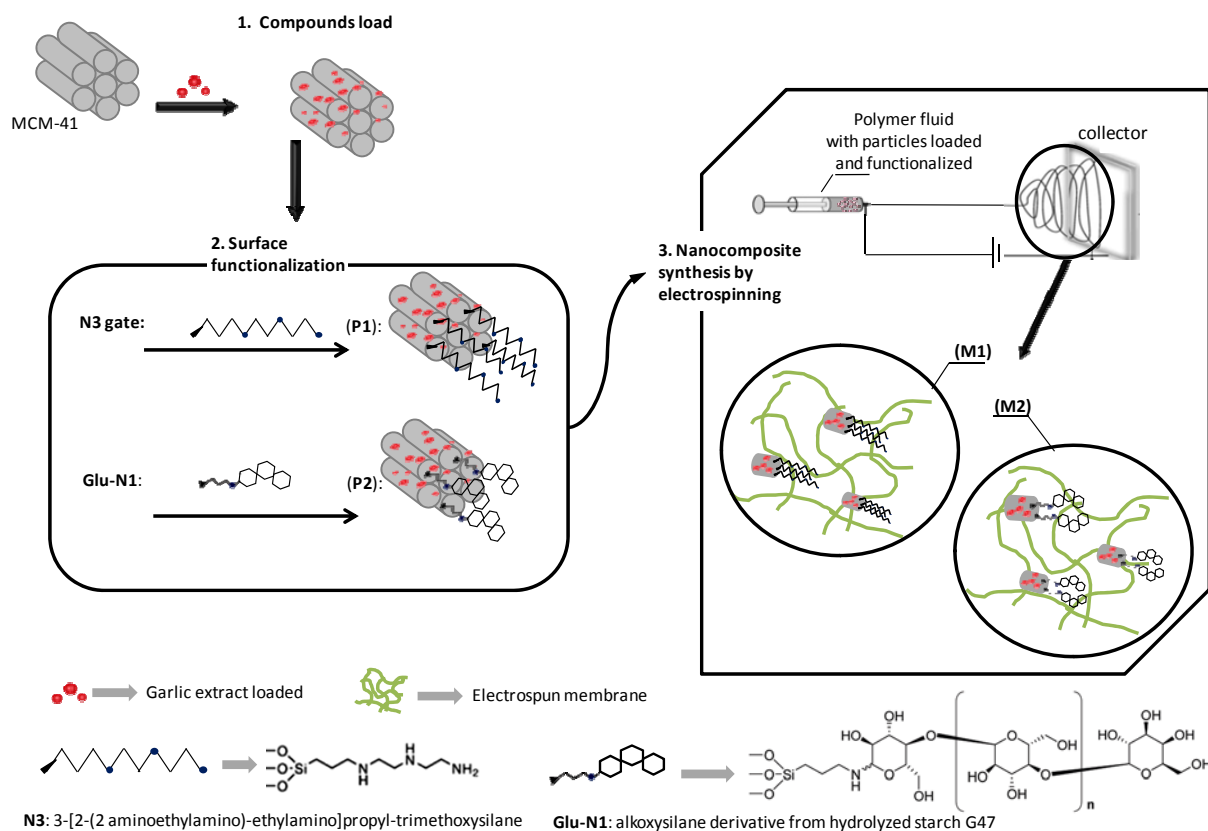
**Scheme 1**. Synthesis of mesoporous particles **P1** (capped with **N3**) and **P2** (capped with **Glu-N1**). Preparation of the composites **M1** and **M2** is also shown.

For the synthesis of the pH-responsive gated material (**P1**) the derivative 3-[2-(2 aminoethylamino)-ethylamino]propyl-trimethoxysilane (**N3**) was selected as simple, yet suitable, open-chain molecular pH-responsive system that was anchored through covalent bonds on the pore outlets of the MCM-41 support. For the preparation of the enzyme-responsive material (**P2**) the commercially available hydrolyzed starch Glucidex® 47 was selected. The hydrolyzed starch was properly derivatized, through reaction with 3-aminopropyltriethoxysilane (**N1**), in order to yield the alkoxysilane derivative (**Glu-N1**) which was then anchored on the external surface of the MCM-41 support.[32]

In the **P1** solid changes in the pH control the state of the gate (open or closed). In particular, open-closed cycle relies on protonation/deprotonation processes of the grafted polyamines. At acidic pH, the nitrogen atoms of the polyamines are fully protonated and strong electrostatic repulsions between the grafted polyamines occur. These strong repulsions pushed away the protonated polyamines blocking the pores of the inorganic support and, as a consequence, inhibit cargo release. Also certain anion-controlled outcome is observed because negatively charged anions interact with the positively charged ammonium moieties leading to a more pronounced pore blocking. At neutral pH the polyamines are only partly deprotonated and the electrostatic repulsions are highly diminished. This allow pore opening due to the more flexible conformational of polyamines (when compared with polyammonium) with the subsequent cargo release.

In solid **P2**, the opening mechanism deals with an enzymatic hydrolysis of the grafted starch, which acts as molecular gate. The anchoring of the saccharides inhibits cargo delivery due to the formation, around the pore outlets, of a dense monolayer of starch molecules. In the presence of pancreatin (a pool of enzymes that contain amylase), the $1 \rightarrow 4$ glycosidic bond between β-D-glucoses present in the starch is hydrolyzed with the subsequent uncapping of the pores and cargo delivery. Scheme 2 shows the release mechanism.
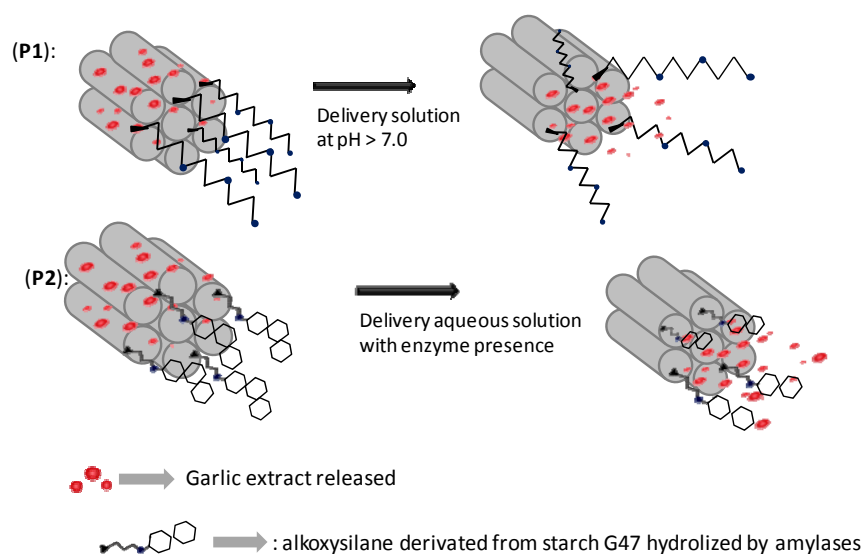
**Scheme 2**. Mechanism of pH and enzyme induce release of the entrapped cargo from **P1** and **P2**.

The composite materials

The final goal of this work was to incorporate the materials **P1** and **P2** on nanofibers as a suitable approach for the development of composite fabrics able to deliver the cargo upon the presence of specific stimuli. Polymer solutions were made based on one of the most standardized protocols.[39-40] Nylon-6 pellets were dissolved in an aqueous solution containing formic acid. The dispersion obtained was stirred for ca. 24 h to make a clear sol–gel. Then 80 mg of solids **P1** or **P2** were added and the mixture was stirred. The final composites **M1** (containing solid **P1**) and **M2** (containing solid **P2**) were obtained by exposition of the prepared mixtures on an electrical field using the well-known electrospinning technique and collected as non-woven membranes on a plate that acts as the counter electrode.[22]

Materials characterization

The characterization of the materials **P1** and **P2** was performed using well-known techniques. Powder X-ray diffraction (PXRD) patterns of the prepared silica mesoporous MCM-41 solids are shown in Figure 1. The PXRD of siliceous as synthesized MCM-41 shows four low-angle

reflections typical of a hexagonal array that can be indexed as (100), (110), (200) and (210). A significant shift of the (100) reflection in the PXRD of the MCM-41 calcined sample is clearly observed (curve b in Figure 1) corresponding to an approximate cell contraction of ca. 5 Å. This displacement and the broadening of the (110) and (200) peaks are most likely related to condensation of silanols during the calcination step, when CTAB is removed. In the case of **P1** and **P2**, the PXRD pattern (curve c and d, in Figure 1) only shows the characteristic (100) reflection. The presence of this peak indicates that the mesoporous structure was preserved through the filling process with the garlic extract and the anchoring of molecular gates.
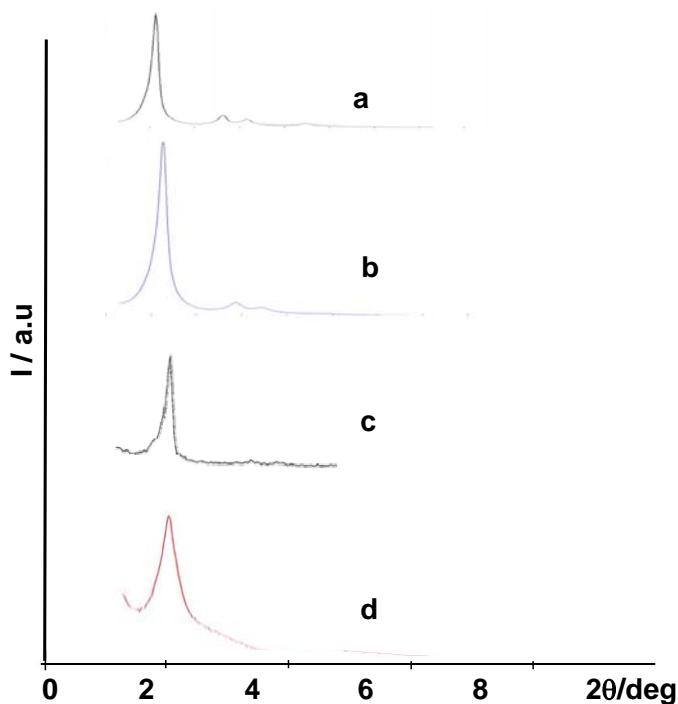


**Figure 1.** Powder X-ray patterns of **a)** as-synthesized MCM-41, **b)** calcined MCM-41, **c)** solid **P2,** and **d)** solid **P1**.

Figure 2 shows TEM images of MCM-41 solid support showing the typical porosity associated with this type of inorganic support. The images also show that the mesoporous solid was obtained as micrometric particles. In fact Dynamic Light Scattering (DLS) studies carried out

with the starting MCM-41 confirmed the presence of micrometric particles with a mean average diameter of ca. 1 μm (see Figure 2).
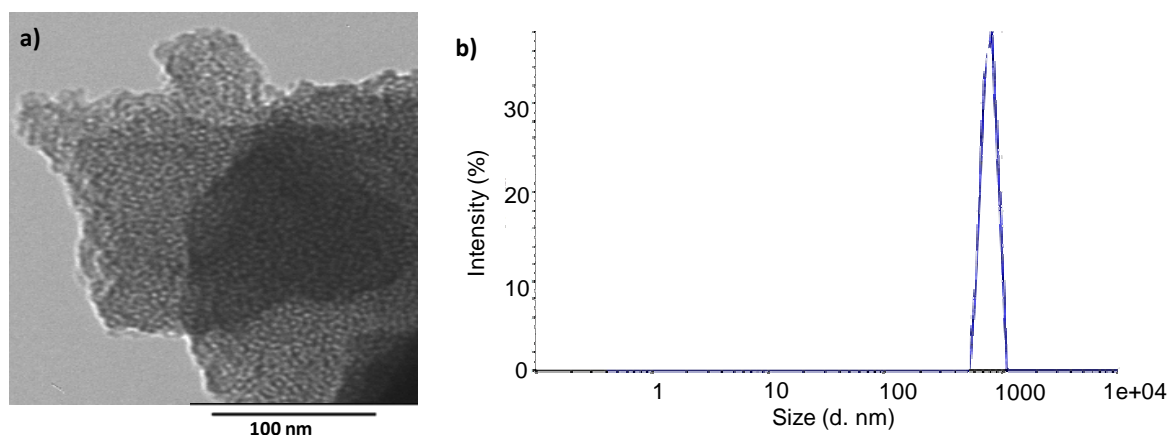


**Figure 2 a)** TEM image of MCM-41 particles and **b)** statistical representation of particle size of MCM-41obtained by DLS (Dynamic Light Scattering) studies.

$N_2$ Adsorption–desorption isotherms of the MCM-41 calcined phase shows typical curves consisting of one single adsorption step at the intermediate $P/P_0$ value (0.1-0.4) which can be related to the nitrogen condensation inside the mesopores by capillarity, as corresponds to a type IV isotherm (see Figure 3). The absence of a hysteresis loop in this interval and the narrow pore distribution suggests the existence of uniform cylindrical mesopores (2.71 nm, 0.88 cm$^3$ g$^{-1}$). The application of the BET model to calcined material gave a value for the total specific surface of 979.6 m$^2$ g$^{-1}$. In contrast, the $N_2$ adsorption–desorption isotherms of the loaded solid **P0** and the final functionalized solids (**P1** and **P2**), show in each case a flat curves with specific surfaces of 220, 100 and 193 m$^2$ g$^{-1}$ and pore volumes of 0.25 0.17 and 0.19 cm$^3$ g$^{-1}$ for **P0**, **P1** and **P2**, respectively. This not only shows an appreciable absence of mesopority but also indicates a significant pore blocking due molecular gates anchorage being as decrease of specific surface and volume pore from solid loaded **P0** to final functionalized solids **P1** and **P2**.

13
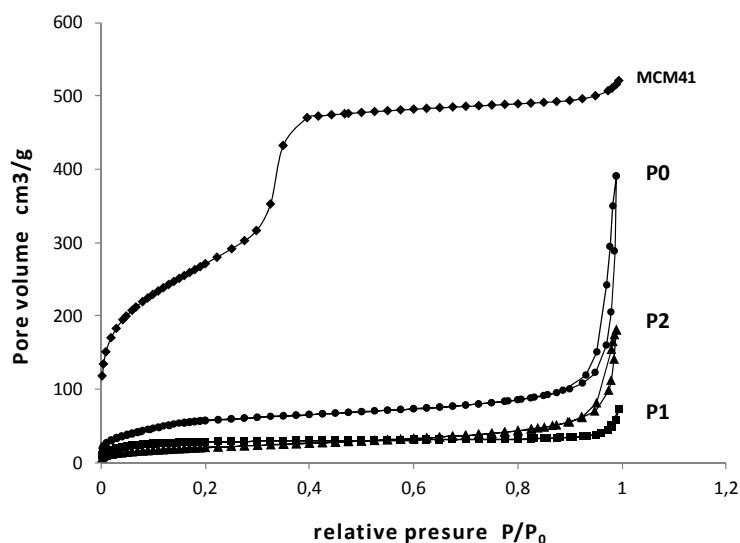
**Figure 3.** Nitrogen adsorption-desorption isotherms: (◆) **MCM-41** calcined material, (●) **P0** solid, (■), **P1** solid, and (▲) **P2** solid.

The organic contents in the loaded solid were determined through thermogravimetric studies. TGA curves showed a weight loss between 100-600 °C due to the organic matter combustion corresponding to the entrapped cargo in **P0** and, in the case of **P1** and **P2**, corresponding to the entrapped cargo and the molecular gate. In particular, the amount of organic matter in the MCM-41 scaffolding loaded with the garlic extract was of ca. 0.18 g garlic extract/g $SiO_2$, whereas the final gated materials **P1** and **P2** have a content of organic matter of 0.38 and 0.25 g/g $SiO_2$, respectively. (See Supporting info S1 for TGA curves).

The morphology of composites **M1** and **M2** was studied by means of FE-SEM. Micrographs of the nanofibrous structures are shown in Figure 4. Nylon-6 ultra-thin fibers, with an average thickness of 160 nm (Figure 4a), exhibited a non-woven arrangement. Several chain entanglements can be observed, which results in a highly porous structure. The absence of beads and fiber bundles indicated that the electrospinning conditions were adequate for a proper and stable solvent evaporation. FE-SEM images of **M1** and **M2** (Figure 4b) show the presence of

entrapped **P1** and **P2** particles, distributed randomly across the nanofibrous matrix. The gated silica particles appear to be partially wrapped in the fibers external surface, suggesting the occurrence of relatively strong adhesive forces.[41] The presence of hydrogen bonding interactions between the polyamide chains of the fibers and the capping molecules covering **P1** and **P2** (polyamines and polysaccharides, respectively) cannot be excluded. The formation of covalent bonds between the fibers and the capping molecules is unlikely considering the preparation conditions for the final **M1** and **M2** composites. It should be noticed that, regardless the nature of the interactions occurring between particles and fibers, the adhesion forces seem to be strong enough for maintaining the composite structure together after the release procedure (Figure 4 c). This was confirmed by FE-SEM-EDX studies that showed the presence of silicon in the composite membranes after release completion, and even after long-term (24h) soaking, in the different release environments tested. (See Supporting info S2 figures for EDX spectra)
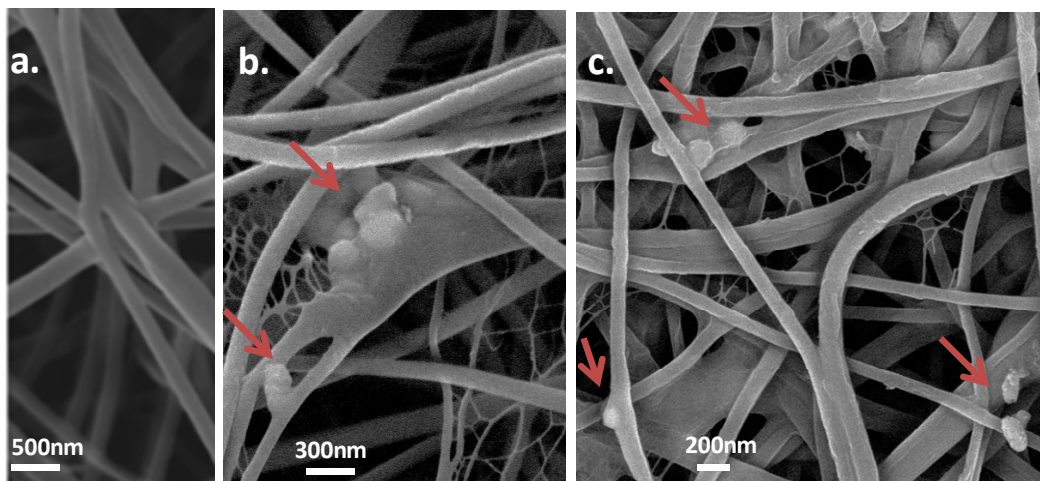


**Figure 4.** Representative FE-SEM images of **a)** nylon6 nanofiber, **b)** composite with entangled microparticles before the released procedure, and **c)** the same composite after the release procedure.

Controlled release behavior

Controlled release studies were performed on **P1**, **P2** and **M1** and **M2**. Cargo delivery was monitored by cyclic voltammetry studies using a reported procedure[37] based in the detection of disulfides (diallyl disulfide – DAD, is one of the major components of the garlic extract) in the presence of bromide. The detection is based on the electrogeneration of bromine on a carbon electrode,[34,37] which reacts with disulfides to catalytically regenerate bromide. This redox reaction induced the appearance of a peak in the voltammogram in the 1.0-1.2 V range,[37] whose intensity is proportional to the amount of disulfides present in the garlic extract. (See Supporting info S3 for Voltammetric evaluations).
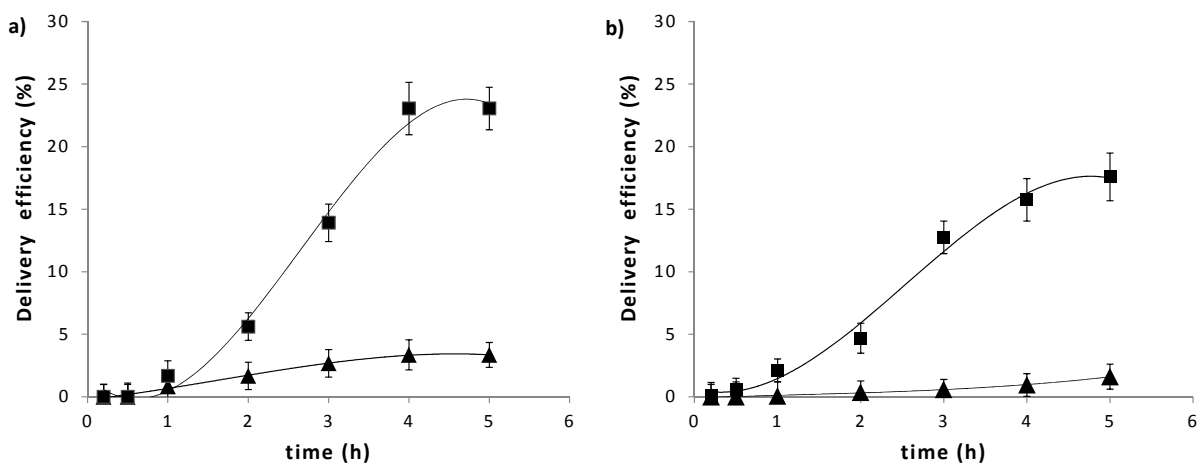


**Figure 5.** Efficiency delivery curves of diallyl disulfide (DAD) in garlic extract from pH-sensitive materials **a) P1** particles and **b) M1** composites. Release at pH 7.0 ( ■ ) and 2.0 ( ▲ ).

In a first step controlled release features of the pH-sensitive materials **P1** and **M1** were evaluated. In a typical experiment 12.5 mg of **P1** or 80 mg of **M1** were suspended in 25 mL of water at pH 2.0 and pH 7.0 (in the presence of sulfates). Then at certain time intervals, fractions of both suspensions were taken and the solid (**P1** or **M1**) was removed. Cargo delivery into the solution was then measured via the electrochemical procedure described above. Diallyl disulfide delivery process was followed by voltammetric responses of the clear solutions. In Figure 5 the

delivery profiles at pH 2.0 and 7.0 for **P1** and **M1** are displayed. The results have been represented as the delivery efficiency, the percentage of the voltammetry signal of each aliquot relative to the signal that would be obtained for the complete delivery of the cargo for each material.

From Figure 5 it can be seen that aqueous suspensions of solid **P1** at pH 2.0 show a poor release of the garlic extract even after some hours in solution (see Figure 5a). This very low release is clearly related with the presence of the polyamine-based gated ensemble. However, when the experiments are carried out in water suspensions at pH 7.0 a release of the cargo is observed as indicated by the time-dependent enhancement of the intensity of the oxidation peak in the 1.0-1.2 V range. In the case of composite **M1**, similar delivery profiles have been obtained this fact clearly indicating that the release process has not been modified when the microcarriers have been dispersed into the membrane. As it can be seen in the FE-SEM images (Figure 4) the particles are not embedded within the fibers but only located on the fiber outer surfaces, so the gated mesopores of the microcarriers are accessible and the opening/closing mechanism is fully operational. However some differences between **P1** and **M1** delivery profiles may be observed. Release from **M1** composite reaches a lower efficiency and the process looks slower, than for **P1** solid. The curve for **M1** does not clearly reach the saturation as it does for **P1** delivery. This fact could be related with some kinetic difficulties for the cargo to be delivered from the **M1** composite due to the intricate morphology of the membrane.
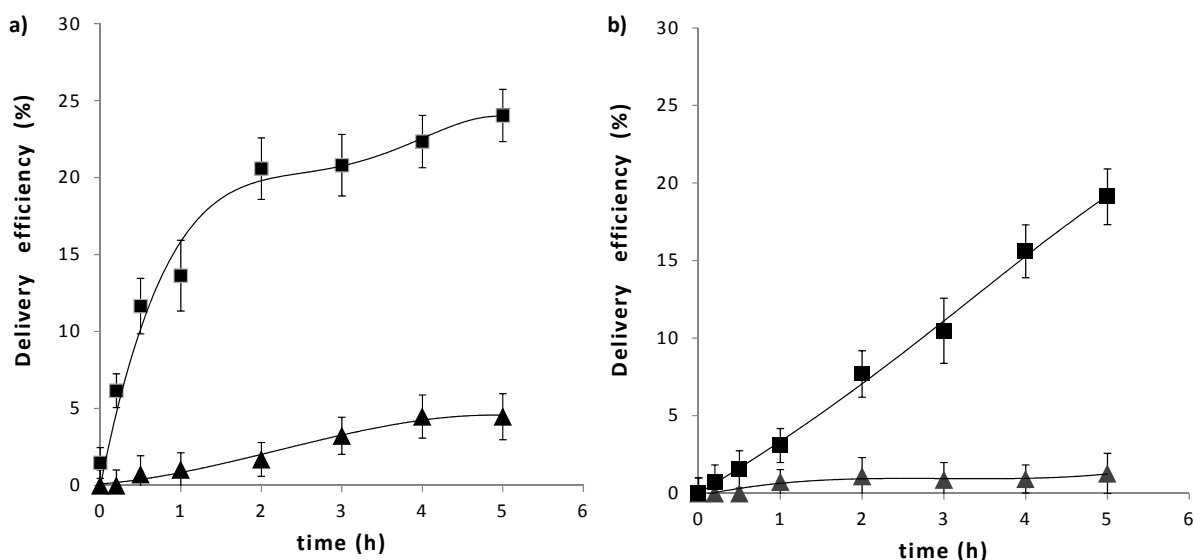
**Figure 6**. Delivery of garlic extract from enzyme-response materials a) **P2** particles and b) **M2** composite. Release in the presence of pancreatine ( ■ ) and release in the enzyme absence ( ▲ ).

Similar delivery experiments were carried out with materials **P2** and **M2**. In particular 12.5 mg of **P2** or 80 mg of **M2** were suspended in 25 mL of water in the presence and in the absence of pancreatin at neutral pH. Then, at a certain time aliquots of both suspensions were taken and the solid materials (**P2** or **M2**) removed. As in the above case cargo release was measured via the electrochemical procedure described previously.

   The delivery profiles for **P2** and **M2** in the presence and absence of pancreatin are displayed in Figure 6. Suspensions of **P2** at neutral pH in the absence of enzyme shows no delivery of the garlic extract which is attributed to the presence of the starch derivative anchored on the external surface of the mesoporous material. In contrast, when the experiments are carried out in the presence of pancreatin a clear release of the cargo is observed and attributed to the enzyme-induced hydrolysis of glycosidic bonds of the grafted polysaccharides. In the case of **M2**, the same basic behavior can be observed, the lack of delivery in the absence of the enzyme and the

18

delivery when the enzyme is present, so the release mechanism may not be affected by the fact of having the micro-carriers embedded into the membrane. However, in this case we can observe a higher difference in the delivery speed for **M2** when comparing with **P2** than for the **P1/M1** system. This, in fact supports the explanation given above for the **M1** behavior. As in the case of **M2** composite the mechanism for opening the gate is more complex than for **M1** because it needs the enzyme to get the micro-carrier surface in order to get the gate open, the intricate morphology of the composite produce a higher effect giving rise to a more pronounced slowdown of the whole process.

This slightly different behavior of the composites **M1** and **M2** respect to the parent **P1** and **P2** materials could be seen as an appropriate method to get a better control of the delivery process, enhancing the closed conditions and allowing a more maintained released of the cargo.


CONCLUSIONS

Two new composite materials (**M1** and **M2**) based on the incorporation of two gated silica mesoporous hybrid solids (**P1** and **P2**) on a electrospun polyamidic nanofiber have been prepared and their controlled release behaviour studied. Those composites presented a fibrous structure with entangled microparticles. At pH 2.0 aqueous suspensions of **M1** showed negligible release of the entrapped extract whereas when the pH is increased to 7.0 a clear cargo delivery from **M1** is observed. In the case of **M2**, the mesoporous gated microparticles are equipped with a polysaccharide able to inhibit cargo release. Addition of pancreatin to aqueous suspensions of **M2** induced cargo delivery due to the progressive enzyme-induced hydrolysis of the grafted polysaccharide. We believe that the development of composite materials based on silica mesoporous microparticles equipped with gate-like systems is an interesting way to prepare

smart fabrics showing "zero" release that can be opened at will using appropriate stimuli. These systems are homogenous and offer an efficient way for the cargo protection, opening a wide range of research opportunities for this delivery concept to be applied in several industries.

AUTHOR INFORMATION

**Corresponding Author**

\* Universidad Politécnica de Valencia, Camino de Vera S/N,

Valencia, Spain. Tel. +34 963877000 Ext: 78258;

E-mail: cararo@upvnet.upv.es.

ACKNOWLEDGMENT

ABBREVIATIONS

**N3**: 3-[2-(2-aminoethylamino)-ethylamino]-propyl-trimethoxysilane **N1:** 3-aminopropyltriethoxysilane, **TEOS**: tetraethylorthosilicate, **CTAB**: n-cetyltrimethylammonium bromide, **TEAH3**: sodium hydroxide, triethanolamine. **Glu-N1**: alkoxysilane derivative of Glucidex 47

Supporting Information Available: Additional information about characterization of materials This material is available free of charge via the Internet at http://pubs.acs.org.

REFERENCES

(1) Hoffmann, F.; Cornelius, M.; Morell, J.; Froba, M.  Silica-Based Mesoporous Organic-Inorganic Hybrid Materials.  *Angew Chem Int Ed Engl* **2006,** *45*, 3216-3251.

(2) Descalzo, A. B.; Martínez-Mañez, R.; Sancenón, F.; Hoffmann, K.; Rurack, K.  The Supramolecular Chemistry of Organic-Inorganic Hybrid Materials.  *Angew Chem Int Ed Engl* **2006,** *45*, 5924-5948.

(3) Aznar, E.; Martínez-Máñez, R.; Sancenón, F.  Controlled Release Using Mesoporous Materials Containing Gate-Like Scaffoldings.  *Expert Opin Drug Deliv* **2009,** *6*, 643-655.

(4) Coti, K. K.; Belowich, M. E.; Liong, M.; Ambrogio, M. W.; Lau, Y. A.; Khatib, H. A.; Zink, J. I.; Khashab, N. M.; Stoddart, J. F.  Mechanised Nanoparticles for Drug Delivery.  *Nanoscale* **2009,** *1*, 16-39.

(5) Coll, C.; Bernardos, A.; Martínez-Manez, R.; Sancenón, F.  Gated Silica Mesoporous Supports for Controlled Release and Signaling Applications.  *Acc Chem Res* **2013,** *46*, 339-349.

(6) Heikkila, T.; Salonen, J.; Tuura, J.; Kumar, N.; Salmi, T.; Murzin, D. Y.; Hamdy, M. S.; Mul, G.; Laitinen, L.; Kaukonen, A. M.; Hirvonen, J.; Lehto, V. P.  Evaluation of Mesoporous TCPSi, MCM-41, SBA-15, and TUD-1 Materials as API Carriers for Oral Drug Delivery.  *Drug Deliv* **2007,** *14*, 337-347.

(7) Carino, I. S.; Pasqua, L.; Testa, F.; Aiello, R.; Puoci, F.; Iemma, F.; Picci, N.  Silica-Based Mesoporous Materials as Drug Delivery System for Methotrexate Release.  *Drug Deliv* **2007,** *14*, 491-495.

(8) Tang, F.; Li, L.; Chen, D.  Mesoporous Silica Nanoparticles: Synthesis, Biocompatibility and Drug Delivery.  *Adv Mater* **2012,** *24*, 1504-1534.

(9)  Kresge, C. T.; Leonowicz, M. E.; Roth, W. J.; Vartuli, J. C.; Beck, J. S.  Ordered

Mesoporous Molecular Sieves Synthesized by a Liquid-Cristal Template Mechanism.

*Nature* **1992,** *359*, 710-712.

(10) Mal, N. K.; Fujiwara, M.; Tanaka, Y.  Photocontrolled Reversible Release of Guest

Molecules from Coumarin-Modified Mesoporous Silica.  *Nature* **2003,** *421*, 350-353.

(11) Agostini, A.; Sancenón, F.; Martínez-Máñez, R.; Marcos, M. D.; Soto, J.; Amorós, P.  A

Photoactivated Molecular Gate.  *Chem Eur J* **2012,** *18*, 12218-12221.

(12) Angelos, S.; Khashab, N. M.; Yang, Y.-W.; Trabolsi, A.; Khatib, H. A.; Stoddart, J. F.;

Zink, J. I.  Ph Clock-Operated Mechanized Nanoparticles.  *J Am Chem Soc* **2009,** *131*,

12912-12914.

(13) Casasús, R.; Climent, E.; Marcos, M. D.; Martínez-Máñez, R.; Sancenón, F.; Soto, J.;

Amorós, P.; Cano, J.  Dual Aperture Control on Ph- and Anion-Driven Supramolecular

Nanoscopic Gate-Like Ensambles.  *J Am Chem Soc* **2008,** *130*, 1903-1917.

(14) Fujiwara, M.; Terashima, S.; Endo, Y.; Shiokawa, K.; Ohue, H.  Switching Catalytic

Reaction Conducted in Pore Void of Mesoporous Material by Redox Gate Control.

*Chem commun.* **2006,** *44*, 4635-4637.

(15) Giri, S.; Trewyn, B. G.; Stellmaker, M. P.; Lin, V. S.-Y.  Stimuli-Responsive Controlled-

Release Delivery System Based on Mesoporous Silica Nanorods Capped with Magnetic

Nanoparticles.  *Angew Chem Int Ed.* **2005,** *44*, 5038-5044.

(16) Fu, Q.; Rao, V. R.; Ista, L. K.; Wu, Y.; Andrzejewski, B. P.; Sklar, L. A.; Ward, T. L.;

López, G. P.  Control of Molecular Transport through Stimuli-Responsive Ordered

Mesoporous Materials.  *Adv Mater* **2003,** *15*, 1262-1266.

(17) Aznar, E.; Mondragón, L.; Ros-Lis, J. V.; Sancenón, F.; Marcos, M. D.; Martínez-Máñez, R.; Soto, J.; Pérez-Payá, E.; Amorós, P. Finely Tuned Temperature-Controlled Cargo Release Using Paraffin-Capped Mesoporous Silica Nanoparticles. *Angew Chem Int Ed Engl.* **2011,** *50*, 11172-11175.

(18) Oroval, M.; Climent, E.; Coll, C.; Erijta, R.; Aviñó, A.; Marcos, M. D.; Sancenón, F.; Martínez-Máñez, R.; Amorós, P. An Aptamer-Gated Silica Mesoporous Material for Thrombin Detection. *Chem commun.* **2013,** *49*, 5480-5482.

(19) Schlossbauer, A.; Kect, J.; Bein, T. Biotin-Avidin as a Protease-Responsive Cap System for Controlled Guest Release from Colloidal Mesoporous Silica. *Angew Chem Int Ed.* **2009,** *48*, 3092-3095.

(20) Park, C.; Kim, H.; Kim, S.; Kim, C. Enzyme Responsive Nanocontainers with Cyclodextrin Gatekeepers and Synergistic Effects in Release of Guests. *J Am Chem Soc* **2009,** *131*, 16614-16615.

(21) Muñoz, B.; Ramila, A.; Pérez-Pariente, J.; Díaz, M.; Vallet-Regí, I. MCM-41 Organic Modification as Drug Delivery Rate Regulator. *Chem Mater.* **2003,** *15*, 500-503.

(22) Arecchi, A.; Scampicchio, M.; Brenna, O. V.; Mannino, S. Biocatalytic Nylon Nanofibrous Membranes. *Anal Bioanal Chem* **2010,** *398*, 3097-3103.

(23) Loh, X. J.; Peh, P.; Liao, S.; Sng, C.; Li, J. Controlled Drug Release from Biodegradable Thermoresponsive Physical Hydrogel Nanofibers. *J Controlled Release* **2010,** *143*, 175-182.

(24) Venugopal, J.; Ramakrishna, S. Applications of Polymer Nanofibers in Biomedicine and Biotechnology. *Appl Biochem Biotechnol* **2005,** *125*, 147-158.

(25) Kriegel, C.; Arecchi, A.; Kit, K.; McClements, D. J.; Weiss, J. Fabrication, Functionalization, and Application of Electrospun Biopolymer Nanofibers. *Crit Rev Food Sci Nutr* **2008,** *48*, 775-797.

(26) Rajesh, V.; Dhirendra, S. K. Nanofibers and Their Applications in Tissue Engineering. *Int J Nanomedicine* **2006,** *1*, 15-30.

(27) Jia, H.; Zhu, G.; Vugrinovich, B.; Kataphinan, W.; Reneker, D. H.; Wang, P. Enzyme-Carrying Polymeric Nanofibers Prepared Via Electrospinning for Use as Unique Biocatalysts. *Biotechnol Prog* **2002,** *18*, 1027-1032.

(28) Price, R. L.; Waid, M. C.; Haberstroh, K. M.; Webster, T. J. Selective Bone Cell Adhesion on Formulations Containing Carbon Nanofibers. *Biomaterials* **2003,** *24*, 1877-1887.

(29) Madhugiri, S.; Dalton, A.; Gutierrez, J.; Ferraris, J. P.; Balkus, K. J., Jr. Electrospun MEH-PPV/SBA-15 Composite Nanofibers Using a Dual Syringe Method. *J Am Chem Soc* **2003,** *125*, 14531-14538.

(30) Zhuang, X.; Cheng, B.; Kang, W.; Xu, X. Electrospun Chitosan/Gelatin Nanofibers Containing Silver Nanoparticles. *Carbohydr Polym* **2010,** *82*, 524-527.

(31) Kim, B. H.; Yang, K. S.; Woo, H. G. Preparation and Electrochemical Properties of Carbon Nanofiber Composite Dispersed with Silver Nanoparticles Using Polyacrylonitrile and Beta-Cyclodextrin. *J Nanosci Nanotechnol* **2011,** *11*, 7193-7197.

(32) Bernardos, A.; Mondragon, L.; Aznar, E.; Marcos, M. D.; Martínez-Manez, R.; Sancenón, F.; Soto, J.; Barat, J. M.; Perez-Paya, E.; Guillem, C.; Amoros, P. Enzyme-Responsive Intracellular Controlled Release Using Nanometric Silica Mesoporous Supports Capped With "Saccharides". *ACS Nano* **2010,** *4*, 6353-6368.

(33) Bernardos, A.; Aznar, E.; Coll, C.; Martínez-Manez, R.; Barat, J. M.; Marcos, M. D.; Sancenón, F.; Benito, A.; Soto, J. Controlled Release of Vitamin B2 Using Mesoporous Materials Functionalized with Amine-Bearing Gate-Like Scaffoldings. *J Control Release* **2008,** *131*, 181-189.

(34) Block, E., *Garlic and Other Alliums*. RSC Publishing: Cambridge, 2010.

(35) Feldberg, R.; Chang, S.; Kotik, A.; Nadler, M.; Neuwirth, Z.; Sundstrom, D.; Thompson, N. In Vitro Mechanism of Inhibition of Bacterialcell Growth by Allicin. *Antimicrob. Agentes Chemother.* **1988,** *32*, 1763-1768.

(36) Cabrera, S.; El Haskouri, J.; Guillem, C.; Latorre, J.; Beltrán, A.; Beltrán, D.; Marcos, M. D.; Amorós, P. Generalised Syntheses of Ordered Mesoporous Oxides: The Atrane Route. *Solid State Sci.* **2000,** *2*, 405-420.

(37) Martindale, B.; Neil, L.; Compoton, R. Towards the Electrochemical Quantification of the Strenght of Garlic. *Analyst* **2011,** *136*, 128-133.

(38) Brunauer, S. E., P.H. Teller, E. Adsorption of Gases in Multimolecular Layers. *J. Am. Chem. Soc.* **1938,** *60*, 309-319.

(39) Granato, F.; Scampicchio, M.; Bianco, A.; Mannino, S.; Bertarelli, C.; Zerbi, G. Disposable Electrospun Electrodes Based on Conducting Nanofibers. *Electroanalysis* **2008,** *20*, 1374-1377.

(40) Arecchi, A.; Scampicchio, M.; Drusch, S.; Mannino, S. Nanofibrous Membrane Based Tyrosinase-Biosensor for the Detection of Phenolic Compounds. *Anal Chim Acta* **2010,** *659*, 133-136.

(41) Xing, M.; Zhong, W.; Xu, X.; Thomson, D. Adhesion Force Studies of Nanofibers and Nanoparticles. *Langmuir* **2010,** *26*, 11809-11814.

Table of content /abstract graphic